

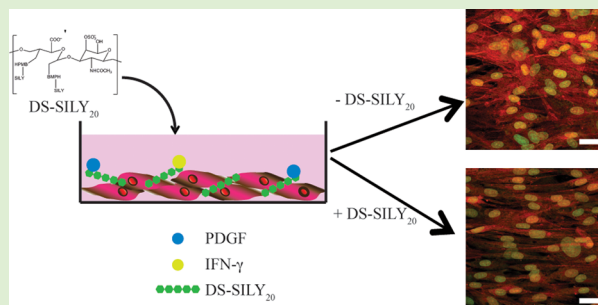
Decorin Mimic Regulates Platelet-Derived Growth Factor and Interferon- γ Stimulation of Vascular Smooth Muscle Cells

Rebecca A. Scott and Alyssa Panitch*

Weldon School of Biomedical Engineering Purdue University, West Lafayette, Indiana 47907, United States

S Supporting Information

ABSTRACT: Following balloon injury, smooth muscle cells (SMCs) serve as targets for many of the pro-inflammatory and pro-fibrotic factors, including platelet-derived growth factor (PDGF) and interferon- γ (IFN- γ) released from activated inflammatory cells and platelets. Previously, our lab designed a mimic of the proteoglycan decorin, termed DS-SILY₂₀, that suppressed vascular SMC proliferation, migration, and protein synthesis in vitro, and injured vessels treated with DS-SILY₂₀ demonstrated reduced hyperplasia in vivo. Here we characterize the effects of DS-SILY₂₀ on modulating PDGF and IFN- γ stimulation in both proliferative and quiescent human SMCs to further evaluate the potential impact of DS-SILY₂₀-SMC interaction on restenosis. Nanomolar dissociation constants were observed between DS-SILY₂₀ and both PDGF and IFN- γ . PDGF significantly increased migration, proliferation, and protein and cytokine expression, as well as increased ERK-1/2 and p38 MAPK phosphorylation in both quiescent and proliferative cultures. However, DS-SILY₂₀ inhibited these increases, presumably through sequestration of the PDGF. Consistent with the complex responses seen with IFN- γ in SMC physiology in the literature, the response of SMC cultures to IFN- γ was variable and complex. However, where increased activity was seen with IFN- γ , DS-SILY₂₀ attenuated this activity. Overall, the results suggest that DS-SILY₂₀ would be an ideal alternative to traditional therapeutics used and may be an effective therapy for the prevention of intimal hyperplasia after balloon angioplasty.



INTRODUCTION

Over the past 10 years, the number of percutaneous coronary intervention (PCI) procedures performed in the United States has increased by 33%.^{1–3} However, thrombosis, neointimal hyperplasia, and restenosis remain complications of this procedure, limiting complete functional recovery of the injured vessel wall. The occurrence of these detrimental consequences following PCI is attributed to trauma during the procedure, which triggers an array of mechanical and biological processes implicated in the healing process. While many different cell types and processes are implicated within the healing response of an injured vessel, previous studies have shown that vascular smooth muscle cells (SMC) activation, migration, and extracellular matrix (ECM) deposition play important roles in intimal hyperplasia.^{4–6}

Following balloon injury, SMCs serve as targets for many of the pro-inflammatory factors released from activated inflammatory cells and platelets, as well as injured endothelial cells and SMCs themselves, stimulating quiescent healthy SMCs to transform to a proliferative synthetic phenotype.^{7–10} Platelet-derived growth factor (PDGF) and interferon- γ (IFN- γ) are two such molecules that activate intracellular transduction pathways, stimulating SMC proliferation, migration, and ECM synthesis, ultimately leading to intimal hyperplasia.^{11–13} PDGF, which has been demonstrated to increase SMC proliferation and migration in vitro and in vivo, as well as upregulate SMC

extracellular matrix synthesis, has been associated with the onset of intimal hyperplasia in arterial-injury models.^{8,14,14,15} While PDGF is pro-stenotic, the function of IFN- γ with respect to regulating SMC activity is more complex, with both pro- and antistenotic activities identified, calling into question the role of the cytokine on SMC proliferation, migration, and protein synthesis.¹⁶ While IFN- γ exhibits conflicting biological activities, the cytokine has a range of influence on disease progression, with recent work providing evidence of an association of IFN- γ with the onset of intimal hyperplasia.¹⁷

In addition to their effects on cell behavior, PDGF and IFN- γ interact with many proteins and proteoglycans within tissues.^{18,19} One such molecule, decorin, a small proteoglycan consisting of a single glycosaminoglycan (GAG) side chain linked to a core protein, plays a significant role in the regulation of SMC migration, proliferation, and extracellular matrix synthesis.^{19–22} Decorin acts through several different mechanisms to regulate cellular activity, either directly, by upregulating cyclin-dependent kinase inhibitors, or indirectly, via interactions with growth factors, such as transforming growth factor- β (TGF- β) and PDGF, which inhibit the biological activity associated with these molecules.^{19,23–25}

Received: February 12, 2014

Revised: April 15, 2014

Published: May 8, 2014

While a large focus has been on the interactions of the protein core with cells, proteins, and signaling molecules,^{26,27} the GAG side chain, typically composed of dermatan sulfate (DS), also contributes to the biological activity associated with the proteoglycan.^{28,29} DS binds to a variety of cytokines and growth factors, including PDGF, TGF- β , and IFN- γ , among others, and these interactions have been shown to alter the effects of the signaling molecules on cell behavior.^{30–33}

Previously, our lab designed a mimic of the decorin proteoglycan.^{34,35} This mimic, termed DS-SILY₂₀, which consists of type I collagen-binding peptides bound to a dermatan sulfate (DS) backbone, has been shown to specifically bind to type-I collagen, serving as a barrier to platelet adhesion and activation in vitro and in vivo.^{35,36} Recently, we demonstrated that DS-SILY₂₀ directs SMC behavior in a manner similar to that of decorin; specifically, DS-SILY₂₀ is able to control SMC migration, protein synthesis, cytokine secretion, and vascular injury marker production of both proliferative and quiescent SMCs in vitro.³⁶ Furthermore, we examined the effects of this molecule on intimal hyperplasia in Ossabaw swine, demonstrating reduced hyperplasia in injured vessels treated with DS-SILY₂₀.³⁶

As both decorin, as well as DS alone, are known to interact with many growth factors involved in the healing process following vessel injury, we asked the question of whether DS-SILY₂₀, which was designed to mimic many of the functions of decorin, also acted through these mechanisms. In this work, we investigated the ability of DS-SILY₂₀ to modulate SMC behavior through interactions with PDGF and IFN- γ . We demonstrate here the ability of DS-SILY₂₀ to interact with both PDGF and IFN- γ . Moreover, we examine how the interaction between DS-SILY₂₀ and PDGF or IFN- γ influences the effects of these chemical stimuli on SMC proliferation, migration, protein synthesis, cytokine secretion, and vascular injury marker production in both proliferative and quiescent SMCs in vitro.

■ EXPERIMENTAL SECTION

DS-SILY₂₀ Synthesis. The decorin mimic (DS-SILY₂₀) was synthesized as previously described.³⁵ Briefly, vicinal diol groups present on the backbone of dermatan sulfate (DS, MW 46 275 Da, Celsus Laboratories) were oxidized via standard periodate oxidation to form aldehyde moieties. Oxidized DS was then covalently coupled to the heterobifunctional cross-linker *N*-[β -maleimidopropionic acid] hydrazide, trifluoroacetic acid salt (BMPH, Thermo Fisher Scientific) in phosphate buffered saline (PBS). The collagen-binding peptide sequence RRANAALKAGELYKSILYGC (noted as SILY, Genscript), derived from the platelet receptor to type I collagen, was conjugated to the DS-BMPH compound; specifically, the thiol group on the cysteine amino acid reacted with the maleimide group of BMPH to form a thioether bond. Purifications were performed at each step by size exclusion chromatography and the number of attached peptides was determined by the consumption of BMPH in the second reaction step. The final product DS-SILY_{*n*}, where *n* indicates the number of attached SILY peptides, was purified in ultrapure H₂O, lyophilized and stored at –20 °C until use. A biotin-labeled version of the decorin mimic was also synthesized by reacting 1 mol of SILY_{biotin} per mole of DS-BMPH for 1 h, followed by addition of unlabeled SILY to complete the reaction and form DS-SILY_{*n*}-biotin.

Solid Phase Binding Assay. DS-SILY₂₀ was coated (1 μ g/well) onto the surface of a 96-well plate (Nalge Nunc International). Nonspecific binding was blocked with 1% bovine serum albumin (BSA) in binding buffer for 1 h at 37 °C. Varying concentrations of platelet-derived growth factor-BB (PDGF, Peprotech) or interferon- γ (IFN- γ , Peprotech) in PBS containing 1% BSA were added to the DS-SILY₂₀ coated surfaces. After a 3 h incubation at 37 °C, plates were rinsed three times with PBS. PDGF bound to the DS-SILY₂₀-coated

surfaces was detected via biotinylated rabbit anti-PDGF-BB or anti-IFN- γ antibody (Peprotech) for 2 h at room temperature. Following rinsing, samples were incubated with streptavidin-HRP, diluted 1:200 in 1% BSA in PBS, for 10 min at room temperature with shaking. Plates were then rinsed three times with PBS to remove any unbound streptavidin-HRP prior to the addition of 1:1 hydrogen peroxide/tetramethylbenzidine, inducing a colorimetric change. After 20 min of incubation, the reaction was stopped via the addition of 2 N sulfuric acid and absorbance was read at 540 nm.

Cell Culture. Human coronary artery smooth muscle cells (SMC, Invitrogen) were cultured in Media 231 (M231, Invitrogen), supplemented with (all from Invitrogen) 4.9% fetal bovine serum (FBS), 2 ng/mL basic fibroblast growth factor, 0.5% epidermal growth factor, 5 ng/mL heparin, 5 μ g/mL insulin, and 0.2 μ g/mL BSA. Unless otherwise noted, cells were initially seeded at 5×10^4 cells/cm² in Ibidi angiogenesis μ -slide (Ibidi) and allowed to proliferate for 24 h to allow the formation of multilayered cell constructs. Media was removed and cultures were treated either with proliferative media, as described above, or contractile media to induce a quiescent phenotype, for 24 h. Previously, we have demonstrated that the addition of contractile media, consisting of M231 supplemented with 1% FBS and 30 μ g/mL heparin, induced SMCs to transition from a proliferative state to a more differentiated, contractile state due to low serum and introduction of heparin.³⁷ Treatments were applied to the SMC cultures. Cells were used between passage numbers 3 and 8 for all assays and maintained at 37 °C with 5% CO₂.

SMC Metabolic Activity. Cultures were incubated in the presence of 10 ng/mL PDGF or IFN- γ with or without DS-SILY₂₀ for 24 h. The metabolic activity of the cells was determined using the CellTiter 96 AQueous One Solution Cell Proliferation Assay (Promega). Briefly, media was mixed with 3-(4,5-dimethylthiazol-2-yl)-5-(3-carboxymethoxyphenyl)-2-(4-sulfophenyl)-2H-tetrazolium, inner salt (MTS) and cultures were reincubated for 2 h at 37 °C with 5% CO₂. The media containing MTS was then transferred into a 96-well plate and absorbance at 490 nm was measured.

Live/Dead Assay. Cultures were incubated in the presence of 10 ng/mL PDGF or IFN- γ with or without DS-SILY₂₀ for 24 h. To test cytotoxicity of DS-SILY₂₀, SMC viability was analyzed using LIVE/DEAD Viability/Cytotoxicity Assay kit (Invitrogen) according to the manufacturer's instruction. Briefly, cultures were rinsed with PBS following treatment and 50 μ L of mixed solution of 2 μ M Calcein AM and 2 μ M ethidium homodimer-1 was added directly to cells. Following incubation for 30 min at room temperature, fluorescent intensity of the cultures was assessed via spectrophotometer to determine cell viability.

PDGFR β and IFN- γ R1 Phosphorylation. Cells were incubated in the presence of 10 ng/mL PDGF or IFN- γ with or without DS-SILY₂₀ for 60 min prior to washing with ice cold TBS and solubilized in lysis buffer (1% NP-40 Alternative, 20 mM Tris, 137 mM NaCl, 10% glycerol, 2 mM EDTA, 1 mM activated sodium orthovanadate, 10 μ g/mL aprotinin, and 10 μ g/mL leupeptin). Lysates were processed at 4 °C for 30 min prior to centrifugation for 5 min at 2000 \times g to remove membrane components. Sandwich ELISAs (all from R&D systems) were utilized to measure total platelet-derived growth factor receptor- β (PDGFR β), total phosphotyrosine PDGFR β , total interferon- γ receptor-1 (IFN- γ R1), and total phosphotyrosine IFN- γ R1. All assays were performed following the manufacturer's protocol.

Proliferation. Cells were incubated in the presence of 10 ng/mL PDGF or IFN- γ with or without DS-SILY₂₀ for 24 h. The effect of DS-SILY₂₀ on cell proliferation was assessed by determining the number of cells per volume following treatment. Cultures were fixed with 4% formaldehyde and nuclei were stained using SYTOX green (Invitrogen). Cells were visualized using an Olympus FV1000 confocal microscope with 60 \times objective. Scans were completed with a xy area of 512 μ m² and one stack, 14 μ m (1 μ m per step) in the z-direction, was taken at three separate locations in each culture. Cell nuclei were counted, such that cell proliferation was assessed by determining the number of SMC nuclei per volume.

Migration. SMC migration was examined via a modified Boyden chamber, using a polycarbonate filter (8.0 μ m pore size, Corning) to

divide the upper and lower chambers. The lower chamber of each well was filled with serum-free media containing 10 ng/mL PDGF or IFN- γ . SMCs were trypsinized and resuspended in serum-free media with or without varying concentrations of DS-SILY₂₀. Cells (5×10^4 cells/cm²) were added to the upper portion of the transwell chamber and incubated for 5 h at 37 °C. Following incubation, cells were fixed in 4% formaldehyde and nuclei stained with Hoechst 33342. Transwells were then mounted on glass slides and migratory SMCs visible on the lower side of the filters were counted by light microscopy using 10 \times magnification.

Protein Synthesis. Cells were incubated in the presence of 10 ng/mL PDGF or IFN- γ with or without DS-SILY₂₀ for 24 h. To determine the effects of DS-SILY₂₀ on protein synthesis in both proliferative and differentiated SMC cultures, click chemistry was utilized to fluorescently label newly synthesized proteins.³⁸ After washing the cells once with PBS, cells were incubated at 37 °C for 60 min with serum-free media to deplete methionine reserves. Cultures were then supplemented with 1 μ M L-azidohomoalanine (AHA, Invitrogen) in serum-free media for 4 h. Cells were then rinsed with PBS to remove any excess AHA and incubated with coculture media overnight to allow protein production. Cultures were fixed with 4% formaldehyde, permeabilized with 0.25% Triton X-100 in PBS, and blocked with 1% BSA in PBS. To detect the newly synthesized proteins containing AHA, alkyne-labeled Alexa Fluor 594 (AF-594, Invitrogen) was selectively bound via copper-catalyzed azide-alkyne ligation. Cell nuclei were stained using SYTOX green.

Proteins were visualized using an Olympus FV1000 confocal microscope with 60 \times objective. Scans were completed with a xy area of 512 μ m² and one stack, 14 μ m (1 μ m per step) in the z-direction, was taken at three separate locations in each culture. Each stack was taken at the same exposure settings to ensure similar darkness values; cultures lacking AHA-treatment were utilized as controls. ImageJ was used to determine the average fluorescent intensity of each stack based on AF-594 fluorescence. Average fluorescent intensity of each stack was then normalized to the number of cells in the 3D image.

Real-Time PCR. SMC cultures were incubated in the presence of 10 ng/mL PDGF with or without DS-SILY₂₀ for 24 h. Following treatment, total RNA was harvested utilizing a Nucleospin Total RNA Isolation Kit (Clontech) according to the manufacturers' recommendations; to eliminate contamination with genomic DNA, DNase digestion was performed for 15 min. Extracted RNA was quantified via a Nanodrop 2000 spectrophotometer (Thermo Scientific) and reverse transcribed into complementary DNA (cDNA) with a High Capacity cDNA Reverse Transcription Kit (Life Technologies). Real-time PCR (qPCR) was performed on a 7500 Real-Time PCR machine (Applied Biosystems) using the Taqman gene expression assays with the following ID numbers (all from Applied Biosystems): Collagen 1 α 2, Hs00164099_m1; Collagen 3 α 1, Hs00943809_m1; Fibronectin, Hs00365052_m1; and β -actin, Hs99999903_m1. cDNA amplification was performed with an initial denaturation step of 10 min at 95 °C, followed by 40 cycles consisting of 15 s denaturation interval at 95 °C and a 1 min interval for annealing and primer elongation at 60 °C. The point at which PCR product was first detected above a fixed threshold (termed the cycle threshold, C_t), was determined for each sample. Changes in the expression of the target gene were calculated using $2^{-\Delta\Delta C_t}$, where $\Delta\Delta C_t = (C_t^{\text{target}} - C_t^{\beta\text{-actin}})_{\text{sample}} - (C_t^{\text{target}} - C_t^{\beta\text{-actin}})_{\text{control}}$. Three independent PCR reactions were performed for each treatment.

Cytokine Production. Cells were incubated in the presence of 10 ng/mL PDGF or IFN- γ with or without DS-SILY₂₀ for 24 h. Media was removed from the cultures and a Pro-Inflammatory I kit (Meso Scale Discovery) was used to analyze cytokine production of SMCs according to manufacturer's instructions. Briefly, plates were warmed to room temperature and incubated with 25 μ L of samples and standards for 2 h at room temperature with vigorous shaking. The detection antibody was then added to the plate and incubated for 2 h at room temperature with vigorous shaking. After washing three times with PBS with 0.05% Tween-20, 2 \times read buffer was added to the plate and imaged using a Sector Imager 2400A (Meso Scale Discovery). The pro-inflammatory markers interleukin-1 β (IL-1 β), interleukin-6 (IL-6),

and tumor necrosis factor- α (TNF- α) were examined in this study. Data were analyzed using the MSD Discovery Workbench Software.

Thrombomodulin Production. Following treatment with 10 ng/mL PDGF or IFN- γ with or without DS-SILY₂₀ for 24 h, cells were washed twice with ice cold PBS and solubilized in lysis buffer (9 M urea, 4% CHAPS, and phosphatase inhibitor cocktail-1 in Millipore water). Lysates were processed at 4 °C for 30 min prior to centrifugation for 20 min at 18000 \times g to remove membrane components. A BCA assay protein kit (Pierce) was used to quantify total protein. A Vascular Injury Marker I kit (Meso Scale Discovery) was used to analyze thrombomodulin production of SMCs according to manufacturer's instructions. Briefly, plates were warmed to room temperature and incubated with 10 μ L of samples and standards for 2 h at room temperature with vigorous shaking. Following gentle rinsing of the wells, the detection antibody was then added and incubated for 1 h at room temperature with vigorous shaking. After washing three times with PBS with 0.05% Tween-20, 2 \times read buffer was added to the plate and imaged using a Sector Imager 2400A. Data were analyzed using the MSD Discovery Workbench Software.

MAPK Phosphorylation. The phosphorylation of mitogen-activated protein kinases (MAPK), including extracellular signal-related kinase (ERK), c-Jun NH2-terminal kinase (JNK), and p38 MAPK (p38), was examined. Cells were incubated in the presence of 10 ng/mL PDGF or IFN- γ with or without DS-SILY₂₀ for 10 or 60 min prior to washing with ice cold tris buffered saline (TBS) and solubilized in lysis buffer (150 mM NaCl, 20 mM Tris, 1 mM EDTA, 1 mM EGTA, 1% Triton-X-100, plus protease inhibitors and phosphatase inhibitors). Lysates were processed at 4 °C for 30 min prior to centrifugation for 20 min at 18000 \times g to remove membrane components. Phospho-JNK (Thr183/Tyr185), phospho-p38 (Thr180/Tyr182), and phospho-ERK-1/2 (Thr/Tyr: 202/204; 185/187) levels were evaluated using the MAP Kinase Whole Cell Lysate kit (Meso Scale Discovery); Total JNK, p38, and ERK-1/2 were determined via MAP Kinase (Total Protein) Whole Cell Lysate Kit (Meso Scale Discovery), according to manufacturer's instructions. Briefly, plates were warmed to room temperature and incubated with 25 μ L of samples for 3 h at room temperature with vigorous shaking. Following gentle rinsing of the wells, the detection antibody was then added and incubated for 1 h at room temperature with vigorous shaking. After washing three times with TBS, 2 \times read buffer was added to the plate and imaged using a Sector Imager 2400A. Data were analyzed using the MSD Discovery Workbench Software. The relative amount of phosphorylated JNK, p38, and ERK-1/2 were normalized to total JNK, p38, and ERK-1/2 for each sample.

Statistical Analysis. Results are expressed as means \pm standard error. Statistical analysis was performed using SAS software (SAS Institute). All results were analyzed using ANOVA with Tukey HSD posthoc test. The threshold for statistical significance was set at $p < 0.05$.

RESULTS

Solid Phase Binding Assay. To assess the ability of PDGF and IFN- γ to bind to DS-SILY₂₀, a solid phase assay with immobilized DS-SILY₂₀ and increasing amounts of the soluble growth factor was employed. PDGF and IFN- γ interactions with DS-SILY₂₀ were dose-dependent and saturable (Figure 1A,B). The interaction between DS-SILY₂₀ and PDGF or IFN- γ in the solid phase assay was characterized via the Hedborn and Heinegard approach and Scatchard-type plots were drawn (Figure 1A,B, insets).³⁹ Dissociation constant (K_d) values, calculated on the basis of Scatchard graph equations, indicate that PDGF has an affinity of 32.2 ± 5.7 nM for DS-SILY₂₀, while IFN- γ exhibited a lower affinity for the mimic of 55.1 ± 6.9 nM.

Metabolic Activity and Cytotoxicity. To better understand the effects of DS-SILY₂₀ with and without PDGF or IFN- γ on SMC behavior, both proliferative and quiescent SMC cultures were used to assess the injured and uninjured SMC

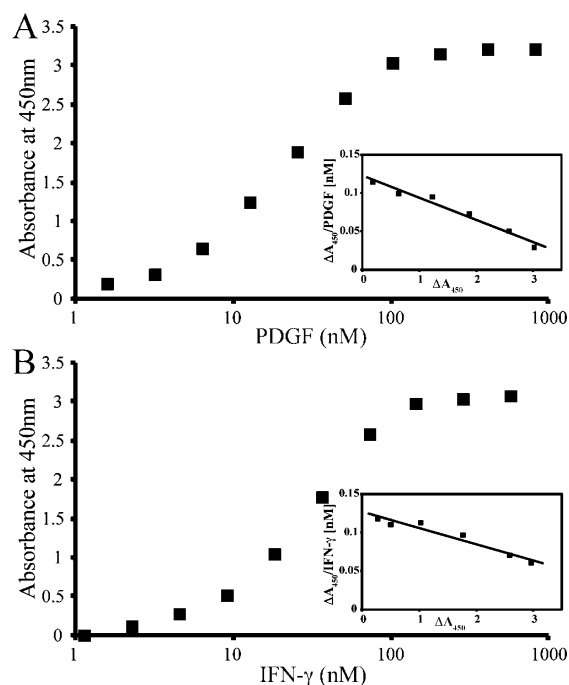


Figure 1. Binding profiles of DS-SILY₂₀ to PDGF and IFN- γ . Saturation binding of (A) PDGF and (B) IFN- γ to DS-SILY₂₀. Immobilized DS-SILY₂₀ was incubated with increasing amounts of PDGF or IFN- γ . The growth factor binding was determined by using biotin-conjugated rabbit-antihuman PDGF or rabbit-antihuman IFN- γ , followed by streptavidin-HRP colorimetric reaction. Insets show a Scatchard-type plot of the experimental data for PDGF and IFN- γ binding to DS-SILY₂₀. Dissociation constants (K_d) were calculated by Scatchard analysis. PDGF binding to particular GAG was analyzed in five experiments. Results of one representative experiment for each GAG are shown.

phenotype, respectively. The different SMC phenotypes were induced via changes in media components, as previously demonstrated elsewhere.³⁷ Using the CellTiter 96 AQ_{ueous} One Solution Cell Proliferation Assay and the LIVE/DEAD Viability/Cytotoxicity Assay, no changes in SMC metabolic activity or viability were exhibited with the addition of PDGF or IFN- γ with any concentration of DS-SILY₂₀ (Figures S1 and S2, Supporting Information). This general trend was demonstrated by both the proliferative and quiescent cultures, as compared to controls.

PDGFR β and IFN- γ R1 Phosphorylation. To assess the ability of DS-SILY₂₀ to modulate PDGF and IFN- γ signaling, phosphorylation of PDGFR β and IFN- γ R1 was investigated. The addition of 10 μ M DS-SILY₂₀ to proliferative or quiescent SMCs did not alter phospho-PDGFR β compared to no treatment controls (Figure 2A,B). Phospho-PDGFR β levels were significantly increased in both proliferative and quiescent SMCs with PDGF treatment. Interestingly, the addition of DS-SILY₂₀ to PDGF-stimulated SMCs resulted in significantly decreased phosphorylation of the PDGF receptor in quiescent cultures compared to cultures stimulated with PDGF alone.

While DS-SILY₂₀ alone did not effect phosphorylation of PDGFR β , the decorin mimic did significantly decrease relative phospho-IFN- γ R1 levels in both proliferative and quiescent cultures compared to no treatment controls (Figure 2C,D). As expected, the addition of IFN- γ to proliferative and quiescent SMCs significantly increased phosphorylation of IFN- γ R1. However, the ability of IFN- γ to induce phosphorylation of its

receptor was significantly hindered when IFN- γ -stimulated cultures were treated with DS-SILY₂₀.

Proliferation. SMC proliferation was assessed by determining the number of SMC nuclei per cell culture volume following the culture period. Similar to previous work, significantly increased numbers of SMC cells were found in proliferative cultures compared to quiescent cultures (Table 1).³⁶ For proliferative SMC cultures, the addition of 10 μ M DS-SILY₂₀ resulted in decreased proliferation compared to controls; however, no change in proliferation was exhibited in quiescent SMC cultures with addition of 10 μ M DS-SILY₂₀.

To examine the influence of DS-SILY₂₀ on SMC-growth factor interactions, the effect of PDGF and IFN- γ on SMC proliferation was further assessed. PDGF added to proliferative cultures induced a significant increase in SMC proliferation. A dose-dependent inhibition of PDGF-stimulated SMC proliferation resulted as the concentration of DS-SILY₂₀ increased in proliferative cultures; ultimately culminating with a 23% decrease in proliferation, compared to PDGF-stimulated SMCs. Interestingly, the addition of IFN- γ to proliferative cultures did not alter SMC proliferation. However, as the concentration of DS-SILY₂₀ increased in IFN- γ -stimulated proliferative cultures, a reduction in proliferation was still observed, with cultures treated with 10 μ M DS-SILY₂₀ displaying a significant reduction in proliferation compared to no treatment controls.

The impact of PDGF and IFN- γ on quiescent SMCs, both in the presence and absence of DS-SILY₂₀, was also probed. A significant increase in SMC proliferation was observed when cultures were treated with either PDGF or IFN- γ , as compared to no treatment controls. Moreover, again a dose-dependent inhibition of SMC proliferation resulted as the concentration of DS-SILY₂₀ increased in cultures treated with either PDGF or IFN- γ . The addition of 0.1, 1, or 10 μ M DS-SILY₂₀ to PDGF-stimulated SMCs resulted in significantly decreased proliferation compared to no treatment controls. Conversely, even at the highest concentration of DS-SILY₂₀, IFN- γ -stimulated SMC proliferation remained significantly increased compared to no treatment controls. However, in cultures treated with 10 μ M DS-SILY₂₀, IFN- γ induced proliferation was significantly reduced by 36% compared to quiescent cultures treated IFN- γ alone.

Migration and Cell Morphology. SMC migration was examined using a modified Boyden chamber.⁴⁰ Similar to previous work, significantly increased migration was exhibited by SMCs in a proliferative phenotype compared to SMCs in a contractile phenotype (Figure 3).³⁶ Furthermore, the addition of 10 μ M DS-SILY₂₀ resulted in significantly reduced migration in both proliferative and quiescent SMCs. The effect of DS-SILY₂₀ on growth factor-stimulated SMC migration was also examined. Proliferative SMCs incurred a significant increase in migration with PDGF treatment (Figure 3A). However, the addition of DS-SILY₂₀ caused a dose-dependent inhibition of PDGF-stimulated SMC migration in proliferative SMCs, where PDGF-stimulated cultures treated with 10 μ M DS-SILY₂₀ exhibited a 94% decrease in migration compared to proliferative SMCs stimulated with PDGF alone. Furthermore, proliferative PDGF-stimulated SMCs treated with 1 or 10 μ M DS-SILY₂₀ demonstrated decreased migration to a level similar to that of quiescent SMCs. Interestingly, the addition of IFN- γ to proliferative cultures did not alter SMC migration (Figure 3B). However, as the concentration of DS-SILY₂₀ increased in IFN- γ -stimulated cultures, SMC migration was still inhibited in

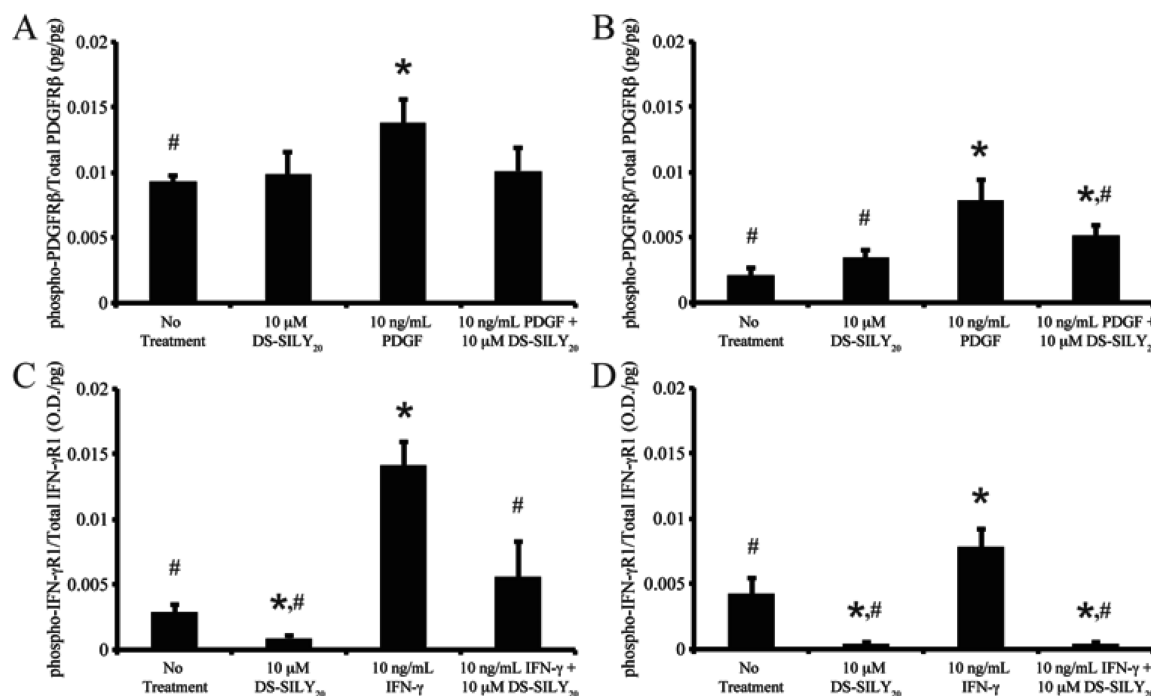


Figure 2. DS-SILY₂₀ regulates phosphorylation of PDGF or IFN- γ receptors in stimulated SMCs. Relative phosphorylated (A, B) PDGFR β or (C, D) IFN- γ R1 produced in (A, C) proliferative and (B, D) quiescent SMCs treated with 10 ng/mL (A, B) PDGF or (C, D) IFN- γ with or without DS-SILY₂₀. The relative amount of phosphorylated PDGFR β and IFN- γ R1 was normalized to total PDGFR β and IFN- γ R1 for each sample, respectively. * Represents significance from control nontreated cells; # Represents significance either PDGF- or IFN- γ -treated cultures ($N > 3$).

Table 1. Proliferation and Protein Expression of Proliferative and Quiescent SMCs Treated with PDGF or IFN- γ and DS-SILY₂₀

treatment	proliferation (cells/mm ³)		protein expression (fluorescence/cell ($\times 10^3$))	
	proliferative SMC	quiescent SMC	proliferative SMC	quiescent SMC
no treatment	15.3 \pm 0.7 ^b	6.8 \pm 0.4 ^{b,c}	71.7 \pm 4.8 ^{b,c}	34.1 \pm 1.8 ^{b,c}
10 μ M DS-SILY ₂₀	11.5 \pm 1.3 ^b	6.2 \pm 0.5 ^{b,c}	59.9 \pm 5.0 ^{a,b}	32.8 \pm 1.3 ^{b,c}
10 ng/mL PDGF + μ M DS-SILY ₂₀				
0	19.1 \pm 1.2 ^a	9.6 \pm 0.8 ^a	86.3 \pm 10.3 ^a	45.3 \pm 4.3 ^a
0.01	17.9 \pm 1.7 ^a	8.9 \pm 0.8 ^a	78.9 \pm 3.8 ^a	33.3 \pm 2.7 ^b
0.1	16.9 \pm 0.8 ^b	7.9 \pm 0.6 ^b	72.3 \pm 4.7	28.7 \pm 3.5 ^b
1	15.8 \pm 1.2 ^b	7.4 \pm 0.3 ^b	68.4 \pm 4.6 ^b	26.2 \pm 2.3 ^{a,b}
10	14.8 \pm 1.4 ^b	6.9 \pm 0.7 ^b	63.3 \pm 3.7 ^b	23.0 \pm 2.6 ^{a,b}
10 ng/mL IFN- γ + μ M DS-SILY ₂₀				
0	15.1 \pm 1.1	9.3 \pm 1.0 ^a	55.0 \pm 9.4 ^a	61.5 \pm 4.3 ^a
0.01	14.3 \pm 2.7	9.2 \pm 0.6 ^a	55.5 \pm 8.3 ^a	52.9 \pm 7.4 ^a
0.1	14.2 \pm 0.8	9.0 \pm 0.7 ^a	49.1 \pm 4.2 ^a	53.4 \pm 2.5 ^{a,c}
1	14.8 \pm 1.1	8.8 \pm 0.9 ^a	45.5 \pm 5.6 ^a	45.4 \pm 4.3
10	13.5 \pm 0.6 ^a	8.1 \pm 1.1	42.4 \pm 4.5 ^a	39.4 \pm 1.6 ^{a,c}

^aSignificance from no treatment control cultures. ^bSignificance from PDGF-stimulated SMC cultures. ^cSignificance from IFN- γ stimulated SMC cultures.

a dose-dependent manner, where cultures treated with 0.1, 1, and 10 μ M DS-SILY₂₀ displayed a significant reduction in migration compared to both no treatment controls and proliferative cultures treated with IFN- γ alone.

Similar to proliferative SMCs, the addition of PDGF to quiescent SMC cultures resulted in a significant increase (~ 5 -fold) in SMC migration compared to no treatment controls (Figure 3C). Likewise, exposure of IFN- γ to quiescent SMC cultures also resulted in a significant increase in SMC migration compared to no treatment controls (Figure 3D). A significant decrease in SMC migration was also observed in PDGF- or IFN- γ -stimulated quiescent SMCs treated with 10 μ M DS-SILY₂₀; however, no change in the number of migratory SMCs

was observed at lower concentrations of DS-SILY₂₀ when cells were stimulated with either PDGF or IFN- γ .

Consistent with altered cell migration, changes in cell morphology were also observed. Proliferative SMCs exhibited a more unorganized, rhomboid-like morphology, which was further intensified by treatment with PDGF and IFN- γ (Figure S3, Supporting Information). However, the addition of DS-SILY₂₀ to proliferative cultures resulted in more aligned, spindle-like SMCs, similar to that of quiescent SMCs. The addition of PDGF and IFN- γ to quiescent cultures resulted in SMCs exhibiting unorganized, rhomboid-like morphological features. DS-SILY₂₀ treatment to PDGF- or IFN- γ -stimulated quiescent SMCs resulted in more organized, spindle-like SMCs.

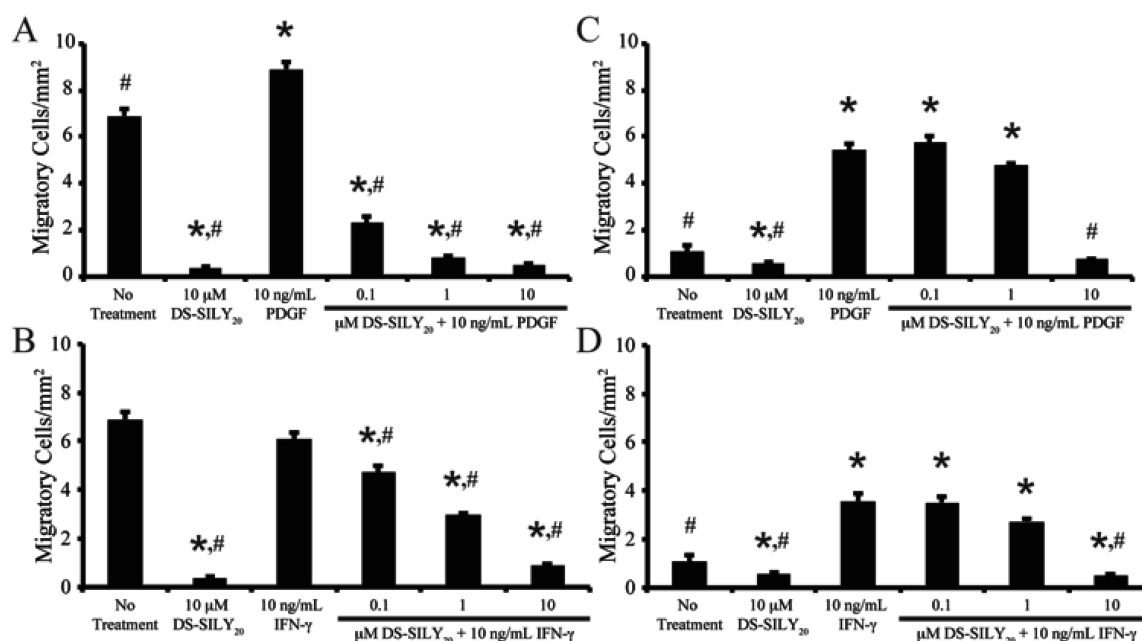


Figure 3. DS-SILY₂₀ regulates PDGF- or IFN-γ-induced SMC migration. Migration of (A, B) proliferative and (C, D) quiescent SMCs treated with 10 ng/mL (A, C) PDGF or (B, D) IFN-γ with or without DS-SILY₂₀. SMC migration was examined via a modified Boyden chamber, where SMCs were treated with PDGF or IFN-γ with or without DS-SILY₂₀. Following incubation, cells were fixed formaldehyde and nuclei stained with Hoechst, to identify migratory SMCs. * Represents significance from control nontreated cells; # represents significance either PDGF- or IFN-γ-treated cultures ($N > 6$).

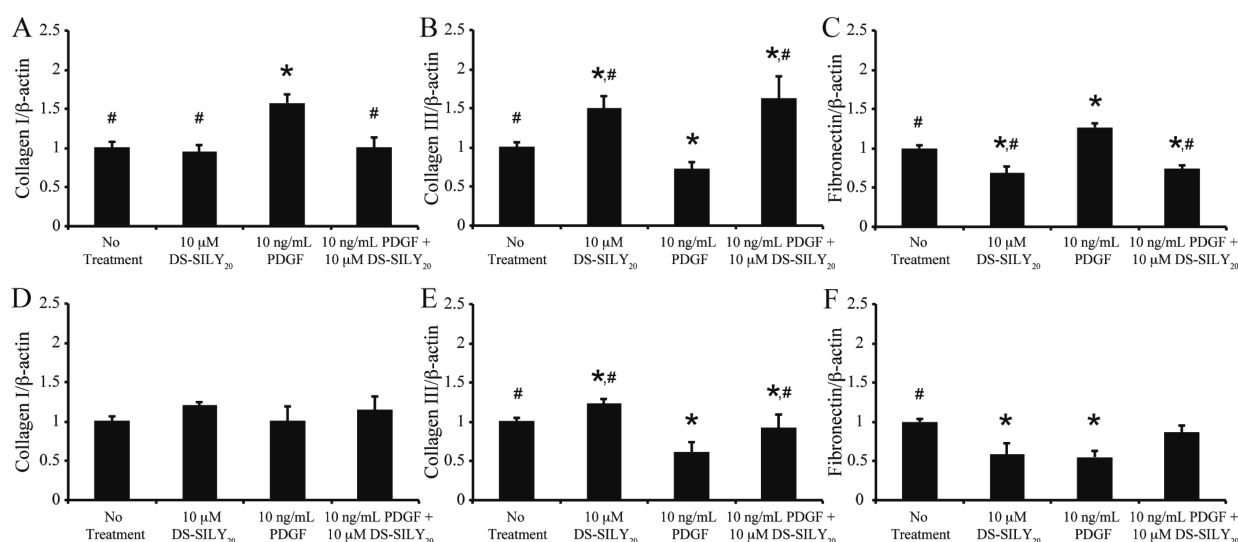


Figure 4. SMC matrix gene expression altered with PDGF and DS-SILY₂₀. Genetic expression of (A, D) collagen I, (B, E) collagen III, and (C, F) fibronectin in (A–C) proliferative and (D–F) quiescent SMCs in response to treatment with PDGF and DS-SILY₂₀. Data normalized to no treatment controls. * Represents significance from control nontreated cells; # represents significance either PDGF-treated cultures ($N > 3$).

Protein Synthesis. As excess protein synthesis is also implicated in intimal hyperplasia, de novo protein synthesis following DS-SILY₂₀ treatment, and doping with AHA, was analyzed by detecting the presence of the incorporated AHA within proteins via copper-catalyzed click chemistry reaction, which attached a fluorescent tag directly to the unnatural amino acid. By quantification of fluorescent intensity, proliferative SMC cultures were found to synthesize approximately ~2-fold more protein compared to quiescent cultures (Table 1). In proliferative SMC cultures, a significant decrease in protein expression was observed in cultures treated with 10 µM DS-SILY₂₀, where approximately 17% less protein was synthesized

compared to control proliferative cultures; protein synthesis in quiescent cultures was not altered with the addition of 10 µM DS-SILY₂₀.

The effect of DS-SILY₂₀ on growth factor-stimulated protein synthesis from proliferative and quiescent SMCs was also probed. Treatment with PDGF significantly increased protein synthesis for SMCs exhibiting a proliferative phenotype. The addition of DS-SILY₂₀ to PDGF-stimulated cultures triggered a dose-dependent inhibition of protein expression in proliferative SMCs, ultimately culminating in a 27% decrease in protein synthesis compared to proliferative SMCs treated with PDGF alone. Moreover, proliferative cultures treated with high

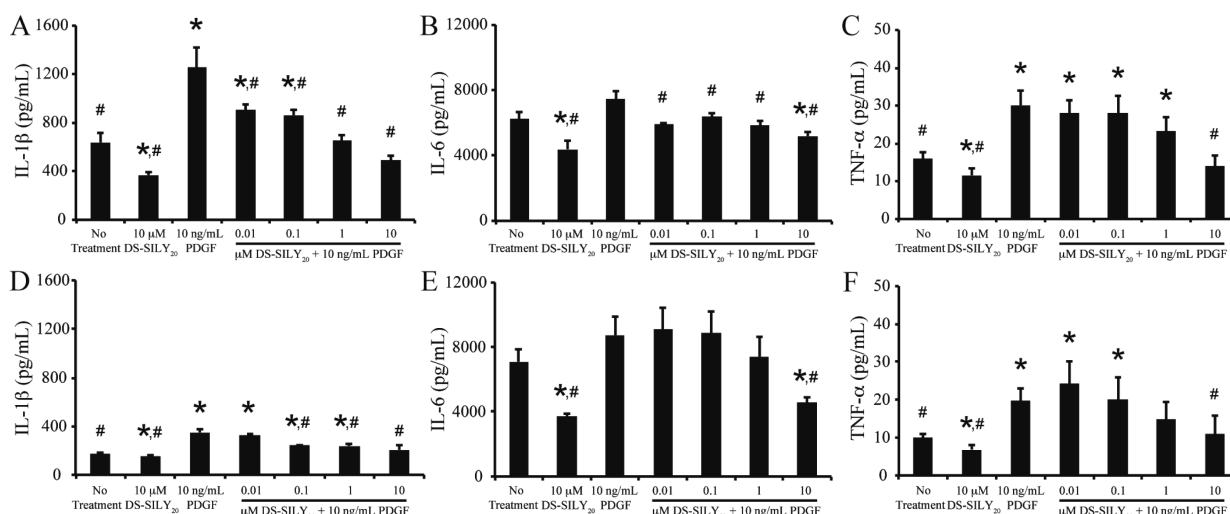


Figure 5. DS-SILY₂₀ attenuates PDGF stimulated cytokine secretion in SMCs. Expression of (A, D) IL-1 β , (B, E) IL-6, and (C, F) TNF- α from (A, B, C) proliferative and (D, E, F) quiescent SMCs in response to 10 ng/mL PDGF with or without DS-SILY₂₀. Cytokines produced by cultured SMCs were measured 24 h post-treatment via. * Represents significance from control nontreated cells; # represents significance either PDGF-treated cultures ($N > 6$).

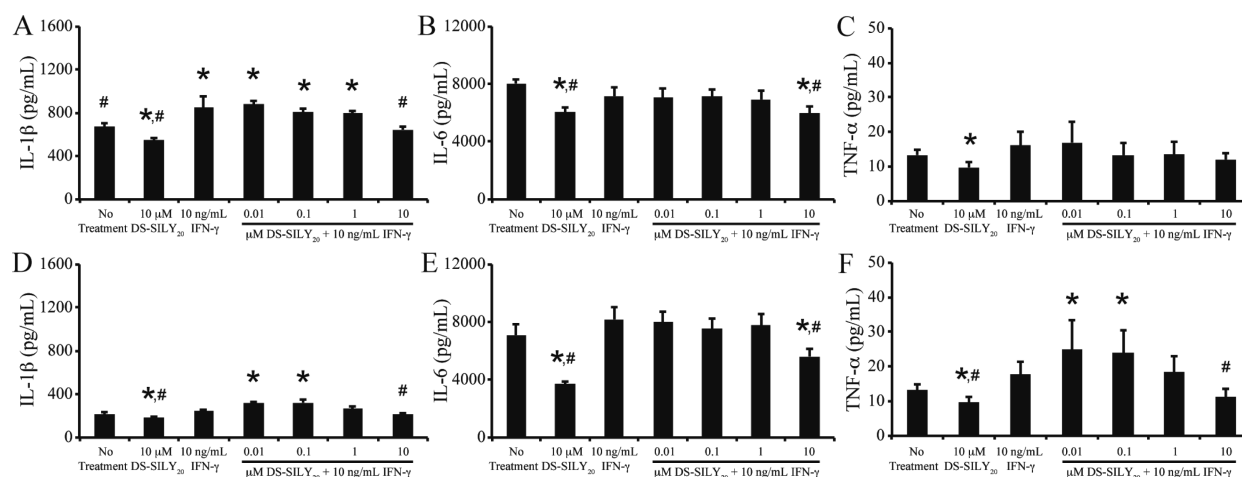


Figure 6. DS-SILY₂₀ controls IFN- γ stimulated cytokine SMC production. Expression of (A, D) IL-1 β , (B, E) IL-6, and (C, F) TNF- α from (A, B, C) proliferative and (D, E, F) quiescent SMCs in response to 10 ng/mL IFN- γ with or without DS-SILY₂₀. Cytokines produced by cultured SMCs was measured 24 h post-treatment. * Represents significance from control nontreated cells; # represents significance either IFN- γ -treated cultures ($N > 6$).

concentrations of DS-SILY₂₀ synthesized protein quantities similar to no treatment controls. Unlike PDGF, the addition of IFN- γ to proliferative cultures significantly reduced protein synthesis. The addition of DS-SILY₂₀ to IFN- γ treated proliferative cultures further reduced protein expression; ultimately culminating with a 41% decrease in protein synthesis compared to no treatment controls.

As expected, stimulation of quiescent SMCs with PDGF or IFN- γ resulted in significantly increased protein expression compared to no treatment controls. A dose-dependent decrease in protein expression was observed in PDGF- or IFN- γ -stimulated quiescent SMCs with increasing concentrations of DS-SILY₂₀. PDGF-induced protein synthesis was significantly decreased in quiescent SMCs treated with any concentration of DS-SILY₂₀ compared to cultures stimulated with PDGF alone. Likewise, protein expression was significantly decreased with the addition of 0.1, 1, or 10 μ M DS-SILY₂₀ to IFN- γ -stimulated cultures compared to quiescent SMCs treated with IFN- γ alone. Furthermore, at the highest DS-SILY₂₀ concentrations

utilized, PDGF-stimulated protein expression was significantly inhibited, as compared to quiescent no treatment controls. However, even at the highest concentration of DS-SILY₂₀ utilized, protein synthesis in IFN- γ -stimulated SMCs remained significantly increased compared to no treatment controls.

Genetic Expression of Collagens and Fibronectin.

Increased protein expression was observed in SMC cultures treated with PDGF (Table 1). As collagen I, collagen III, and fibronectin are differentially expressed ECM proteins within intimal hyperplastic tissue, changes in gene expression of these proteins were examined in PDGF and DS-SILY₂₀ treated SMC cultures via qPCR (Figure 4). For proliferative SMC cultures, the addition of DS-SILY₂₀ significantly reduced the expression of fibronectin mRNA and the increased expression of collagen III genes (Figure 4A–C). Proliferative SMC cultures exposed to PDGF demonstrated significant upregulation of collagen I and fibronectin mRNA, while collagen III gene expression levels were downregulated. The reduction of collagen III mRNA expression due to PDGF exposure was circumvented

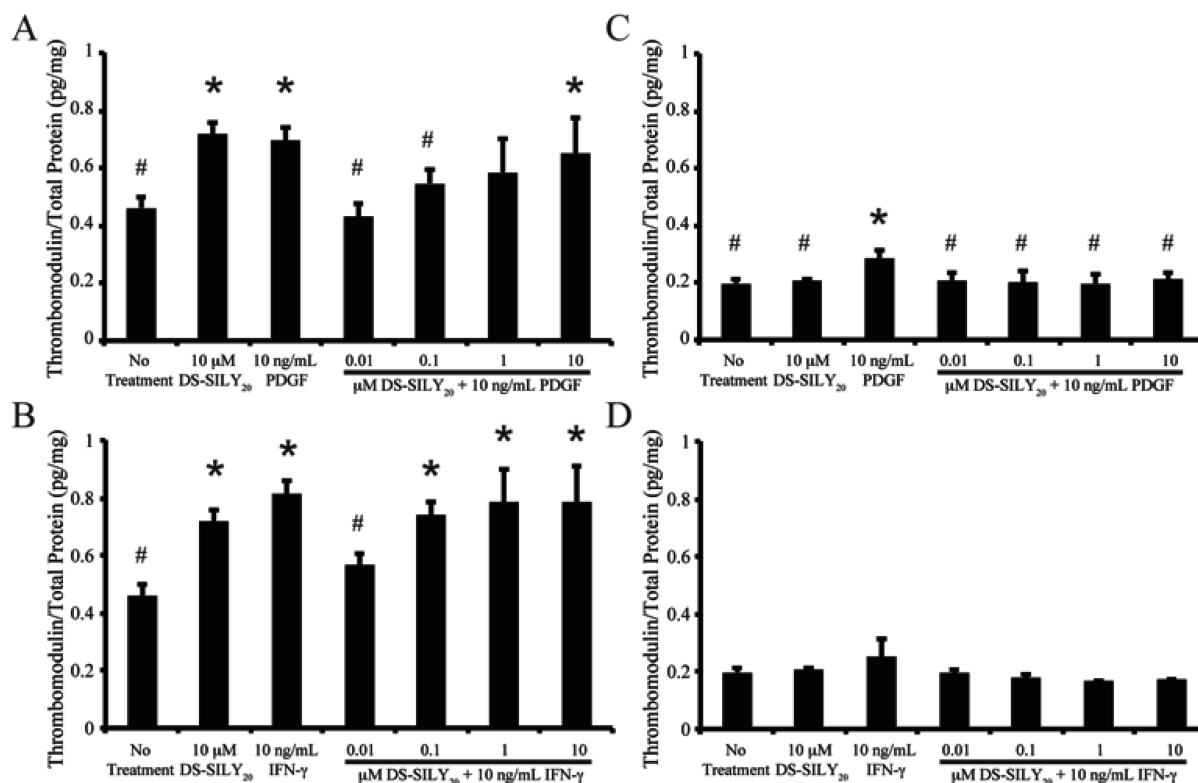


Figure 7. DS-SILY₂₀ regulates PDGF- or IFN-γ-induced SMC thrombomodulin production. Thrombomodulin expression from (A, B) proliferative and (C, D) quiescent SMCs treated with 10 ng/mL (A, C) PDGF or (B, D) IFN-γ with or without DS-SILY₂₀. Thrombomodulin produced by cultured SMCs was measured 24 h post-treatment following cell lysis. * Represents significance from control nontreated cells; # represents significance either PDGF- or IFN-γ-treated cultures (N > 6).

with DS-SILY₂₀ addition, where the genetic expression of collagen III was significantly increased compared to both proliferative controls and SMCs treated with PDGF alone. Furthermore, the addition of DS-SILY₂₀ to PDGF-stimulated cultures significantly decreased expression of fibronectin and collagen I mRNA compared to SMCs treated with PDGF alone.

The genetic expression of collagen I in quiescent SMCs was not altered with DS-SILY₂₀ treatment compared to quiescent no treatment controls; however, the addition of DS-SILY₂₀ significantly increased collagen III gene expression and reduced the expression of fibronectin mRNA (Figure 4D–F). PDGF significantly down-regulated both collagen III and fibronectin mRNA, compared to quiescent no treatment controls. Collagen I gene expression was not altered by the addition of PDGF with or without DS-SILY₂₀ cotreatment. However, when quiescent SMCs were cotreated with PDGF and 10 μM DS-SILY₂₀, collagen III and fibronectin mRNA expression increased compared to cultures exposed to PDGF alone.

Cytokine Production. Following vessel injury, stimulated SMCs actively participate in the inflammatory cascade, producing, and secreting a range of factors, including IL-1β, IL-6, and TNF-α.^{7,8} Thus, expression of IL-1β, IL-6, and TNF-α from SMC cultures following treatment with PDGF or IFN-γ was examined via MSD Sector Imager. Examination of nontreated control cultures revealed that proliferative SMCs exhibited increased levels of IL-1β and TNF-α compared to quiescent cultures; however, the two cultures produced similar levels of IL-6 (Figures 5 and 6). The addition of DS-SILY₂₀ to either SMC cultures exhibiting either phenotype resulted in significant reductions in IL-1β, IL-6, and TNF-α expression.

The effect of DS-SILY₂₀ on the production of pro-inflammatory cytokines following PDGF or IFN-γ stimulation was evaluated in both proliferative and quiescent SMC cultures. PDGF addition to proliferative SMCs significantly increased IL-1β and TNF-α production; however, IL-6 levels did not change compared to controls (Figure 5A–C). A general trend was observed such that as the concentration of DS-SILY₂₀ increased, cytokine production in PDGF-stimulated SMCs decreased, where significant reductions in IL-1β, IL-6, and TNF-α expression were observed at the highest levels of DS-SILY₂₀ tested, compared to proliferative cultures treated with PDGF alone. At 10 μM DS-SILY₂₀, production of IL-1β and TNF-α in PDGF-stimulated cultures was reduced to levels similar to that of no treatment controls, while IL-6 expression was significantly decreased compared to controls. The addition of IFN-γ to proliferative cultures resulted in increased IL-1β production; however, no changes in IL-6 and TNF-α expression were exhibited (Figure 6A–C). When proliferative cultures were cotreated with IFN-γ and DS-SILY₂₀, a dose-dependent inhibition of IL-1β production occurred as the concentration of DS-SILY₂₀ increased. Conversely, DS-SILY₂₀ did not influence TNF-α production in IFN-γ-stimulated proliferative SMCs. Interestingly, IL-6 expression was only significantly decreased in proliferative cultures treated with IFN-γ and 10 μM DS-SILY₂₀.

Similar to proliferative SMCs, the addition of PDGF to quiescent cultures significantly increased IL-1β and TNF-α production; however, IL-6 levels did not change compared to controls (Figure 5D–F). High concentrations of DS-SILY₂₀ mitigated the increase in IL-1β and TNF-α produced from quiescent SMCs exposed to PDGF; however, no change in IL-

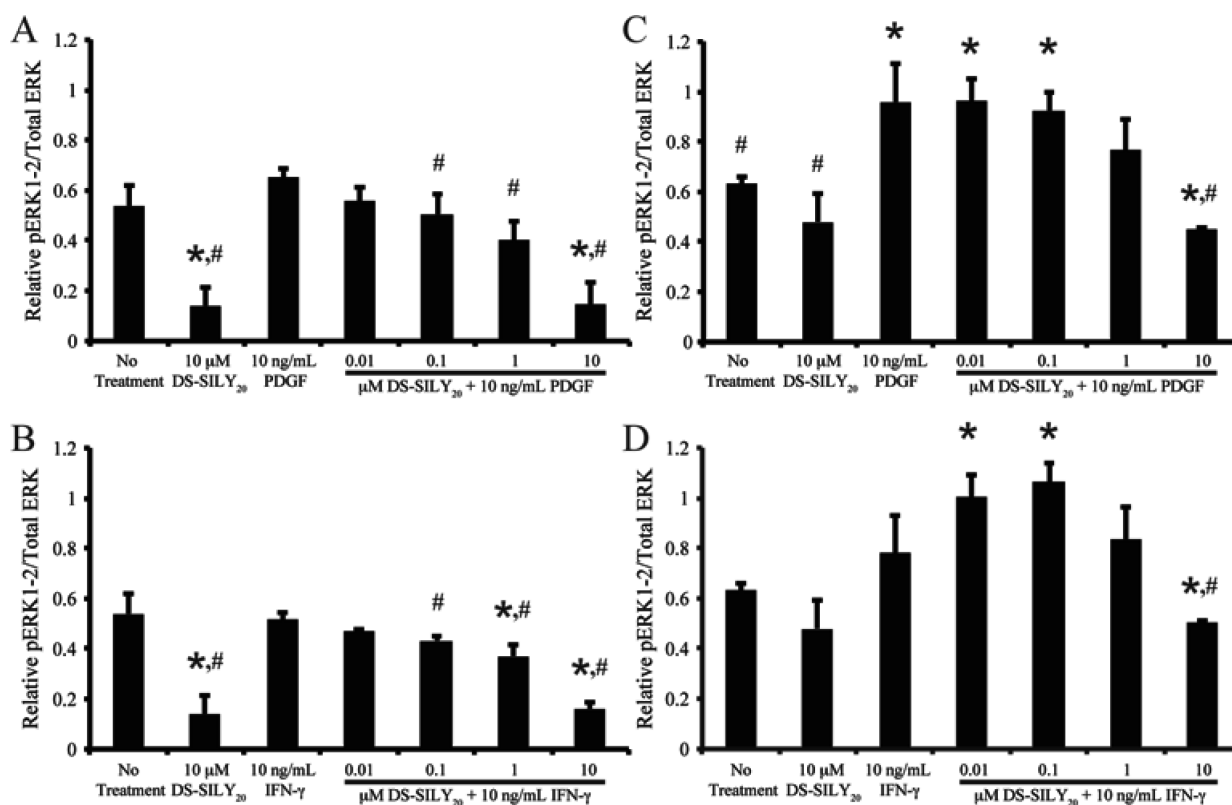


Figure 8. DS-SILY₂₀ regulates PDGF- or IFN- γ -induced ERK-1/2 phosphorylation in SMCs. Relative phosphorylated ERK-1/2 produced in (A, B) proliferative and (C, D) quiescent SMCs treated with 10 ng/mL (A, C) PDGF or (B, D) IFN- γ with or without DS-SILY₂₀. The relative amount of phosphorylated ERK was normalized to total ERK for each sample. * Represents significance from control nontreated cells; # represents significance either PDGF- or IFN- γ -treated cultures ($N > 5$).

1 β and TNF- α expression from PDGF-stimulated cultures was observed at lower concentrations of DS-SILY₂₀, compared to quiescent controls. Cytokine expression was not altered in quiescent SMCs stimulated with IFN- γ alone (Figure 6D–F). However, IL-1 β and TNF- α production in quiescent SMCs significantly increased when cultures were cotreated with IFN- γ and low concentrations of DS-SILY₂₀. However, this effect was mitigated at high concentrations of DS-SILY₂₀, where cytokine production was similar to no treatment controls. IL-6 production in quiescent SMCs was not altered by treatment with IFN- γ , with or without DS-SILY₂₀ cotreatment.

Thrombomodulin Expression. Following vessel injury, the production of thrombomodulin by endothelial cells and SMCs decreases the thrombogenic potential of the damaged tissue. Thrombomodulin produced by SMCs in culture was analyzed via MSD Sector Imager. Control nontreated proliferative SMCs cultures exhibited significantly increased amounts of thrombomodulin compared to quiescent SMC cultures (Figure 7). In proliferative SMC cultures, a significant increase in thrombomodulin production was observed in cultures treated with 10 μ M DS-SILY₂₀; however, thrombomodulin expression in quiescent cultures was not altered with the addition of 10 μ M DS-SILY₂₀.

The addition of PDGF or IFN- γ to proliferative cultures stimulated thrombomodulin production (Figure 7A,B). The addition of 0.01 μ M DS-SILY₂₀ to PDGF- or IFN- γ -stimulated cultures significantly decreased thrombomodulin expression compared to cultures stimulated with either growth factor alone. However, at higher concentrations of DS-SILY₂₀, thrombomodulin expression in PDGF- or IFN- γ -stimulated

SMCs increased to levels similar to proliferative cultures stimulated with growth factor alone.

Quiescent SMCs also exhibited increased thrombomodulin following PDGF stimulation; however, IFN- γ had no effect on thrombomodulin production in quiescent cultures (Figure 7C,D). Interestingly, no change in thrombomodulin production was exhibited in quiescent PDGF-stimulated SMCs with the addition of any concentration of DS-SILY₂₀, compared to no treatment controls. Likewise, thrombomodulin expression was not altered in quiescent SMC cultures cotreated with IFN- γ and DS-SILY₂₀.

MAPK Phosphorylation. MAPKs, including ERK, JNK, and p38, are important intracellular transduction pathways involved in vascular remodeling and disease.^{41–43} To determine the relative amount of phosphorylated ERK-1/2 (pERK-1/2), JNK (pJNK), and p38 (pp38), quiescent and proliferative SMCs were stimulated with 10 ng/mL PDGF or IFN- γ with or without DS-SILY₂₀ for 10 min or 1 h. Cell lysates were then analyzed via MSD Sector Imager to determine the relative phosphorylation levels of the intracellular signaling molecules (Figures 8 and 9). No significant changes in pJNK were observed for any treatments at the time points examined (data not shown).

Phosphorylation of ERK-1/2 has previously been correlated with increased SMC migration.⁴⁴ Thus, we sought to correlate the changes observed in migration (Figure 3) with pERK-1/2 phosphorylation levels. After 10 min of stimulation, the addition of 10 μ M DS-SILY₂₀ to proliferative SMCs significantly decreased pERK-1/2 compared to no treatment controls (Figure 8A). However, pERK-1/2 levels were not

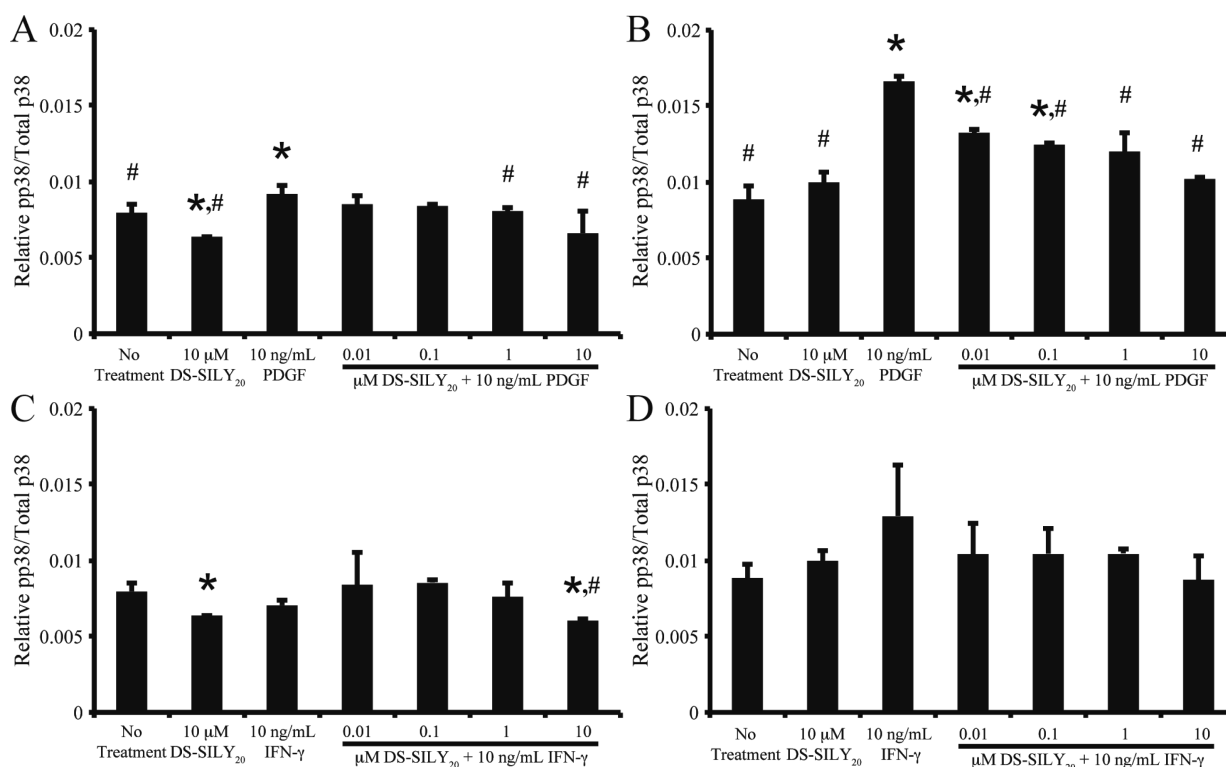


Figure 9. DS-SILY₂₀ attunes p38 phosphorylation in PDGF- or IFN- γ -stimulated SMCs. Relative phosphorylated p38 produced in (A, C) proliferative and (B, D) quiescent SMCs treated with 10 ng/mL (A, B) PDGF or (C, D) IFN- γ with or without DS-SILY₂₀. The relative amount of phosphorylated p38 was normalized to total p38 for each sample. * Represents significance from control nontreated cells; # represents significance either PDGF- or IFN- γ -treated cultures ($N > 5$).

altered with the addition of PDGF to proliferative SMCs. For proliferative cultures, the addition of DS-SILY₂₀ to PDGF-stimulated SMCs resulted in a dose dependent decrease in pERK-1/2 compared to cultures stimulated with PDGF alone. Furthermore, the addition of 10 μ M DS-SILY₂₀ significantly decreased pERK-1/2 levels compared to both no treatment and PDGF-stimulated cultures. The addition of IFN- γ to proliferative cultures did not affect pERK-1/2 levels (Figure 8B). However, as the concentration of DS-SILY₂₀ increased within IFN- γ -stimulated SMCs, a dose dependent decrease of pERK-1/2 was still observed. Interestingly, relative levels of pERK-1/2 in proliferative cultures returned to levels similar to that of no treatment controls after 60 min of stimulation, independent of treatment and phenotype (data not shown).

In contrast to proliferative SMC cultures, after 10 min of treatment pERK-1/2 was not altered in quiescent SMCs dosed with 10 μ M DS-SILY₂₀ treatment (Figure 8C). However, pERK-1/2 was significantly increased in PDGF-treated quiescent cultures compared to no treatment controls. For quiescent cultures, the addition of DS-SILY₂₀ to PDGF-stimulated SMCs resulted in a dose dependent decrease in pERK-1/2 compared to cultures stimulated with PDGF alone. Furthermore, the addition of 10 μ M DS-SILY₂₀ significantly decreased pERK-1/2 levels compared to both no treatment and PDGF-stimulated cultures after 10 min of stimulation. The addition of IFN- γ to quiescent cultures did not affect pERK-1/2 levels (Figure 8D). Interestingly, pERK-1/2 levels in IFN- γ -stimulated quiescent SMCs significantly increased in cultures treated with the lowest concentrations of DS-SILY₂₀ and IFN- γ , compared to no treatment controls. However, as the concentration of DS-SILY₂₀ increased in IFN- γ -stimulated cultures, pERK-1/2 significantly decreased. Similar to results

observed for proliferative cultures, relative levels of pERK-1/2 in quiescent cultures treated with IFN- γ and DS-SILY₂₀ returned to levels similar to that of no treatment controls after 60 min of stimulation; however, elevated levels of pERK-1/2 were still observed in quiescent SMCs stimulated with PDGF alone or PDGF and low concentrations of DS-SILY₂₀ (data not shown).

Several studies have correlated phosphorylation of p38 with increased inflammatory cytokine expression.^{45–47} Thus, we sought to correlate the changes observed in cytokine expression (Figures 5 and 6) with p38 phosphorylation levels. Contrasting results were seen when stimulating with DS-SILY₂₀. The addition of 10 μ M DS-SILY₂₀ to proliferative SMCs significantly decreased pp38 compared to no treatment controls, after 10 min of stimulation, while pp38 was not altered in quiescent SMCs dosed with 10 μ M DS-SILY₂₀ treatment (Figure 9). The addition of PDGF to SMC cultures elicited significant increases in pp38, independent of phenotype, after 10 min (Figure 9A,B). Enhanced pp38 levels, due to PDGF treatment, were mitigated with the addition of DS-SILY₂₀ to either phenotype, where a dose-dependent decrease in pp38 was observed as DS-SILY₂₀ concentrations increased in PDGF-stimulated cultures. The addition of IFN- γ to either proliferative or quiescent SMC cultures did not alter pp38 levels after 10 min of stimulation (Figure 9C,D). The addition of DS-SILY₂₀ to IFN- γ -stimulated quiescent cultures did not alter pp38 levels compared to no treatment controls, even at the highest concentrations of DS-SILY₂₀ utilized. No changes in pp38 levels were exhibited in proliferative SMCs cotreated with IFN- γ and low concentrations of DS-SILY₂₀; however, pp38 levels were significantly reduced in IFN- γ -stimulated cultures treated with 10 μ M DS-SILY₂₀, compared

to no treatment controls. Interestingly, relative levels of pp38 in both proliferative and quiescent cultures returned to levels similar to that of no treatment controls after 60 min of stimulation, independent of treatment and phenotype (data not shown).

DISCUSSION

A detrimental consequence following PCI is injury to the vessel wall during balloon expansion, which triggers an array of mechanical and biological processes, leading to the occurrence of thrombosis, neointimal hyperplasia, and restenosis.⁴⁸ Biochemical stimuli, such as growth factors and cytokines, produced by platelets, inflammatory cells, SMCs, and endothelial cells following vessel injury activate intracellular transduction pathways, stimulating SMC proliferation, migration, and ECM synthesis, ultimately leading to intimal hyperplasia.^{8,11,14} Activated platelets release both PDGF and IFN- γ following vascular injury that occurring during balloon angioplasty. Further, both play important roles in vascular repair, and have been implicated in the development of intimal hyperplasia.^{14,16} Therapeutics able to control SMC proliferation, migration, and ECM production that lead to intimal hyperplasia, and that also allow for endothelium regeneration, are needed to improve outcomes following balloon angioplasty. We have previously demonstrated that DS-SILY₂₀ inhibits platelet binding to vessels walls following balloon angioplasty, and further showed that intimal hyperplasia was reduced 28 days following injury in vivo.³⁶ To further delineate mechanisms through which DS-SILY₂₀ suppresses intimal hyperplasia, we sought to understand the interactions between PDGF or IFN- γ and DS-SILY₂₀ in proliferative and quiescent SMC cultures. We demonstrate here that the antithrombotic biomolecule, DS-SILY₂₀, binds to PDGF and IFN- γ and limits the effects of the growth factors on altered SMC morphology, proliferation, migration, protein synthesis, cytokine secretion, and vascular injury marker production in both proliferative and quiescent SMCs in vitro.

We first set out to assess potential effects of DS-SILY₂₀ on SMCs. No measurable changes in metabolic activity or cell viability were observed in either proliferative or quiescent SMC cultures following PDGF or IFN- γ treatment with and without DS-SILY₂₀ (Figures S1 and S2, Supporting Information). Thus, the inhibitory effect of DS-SILY₂₀ on PDGF- or IFN- γ -stimulated SMC function is likely not attributed to cell death. Rather, the observed changes in cell behavior are likely attributed to the ability of DS-SILY₂₀ to bind with high affinity to both the ECM molecule collagen, and to the growth factors PDGF and IFN- γ , thus effectively sequestering the growth factors in the matrix and attenuating the impact of the growth factors on SMC activity. Others have previously demonstrated that PDGF binds to DS with an affinity ranging between 15 and 91 nM, depending on the source of the DS, and also to decorin at an affinity of ~16 nM.^{30,49} In the present work, the straight-line correlation in the Scatchard-type plots shown for both growth factors (Figure 1A,B, insets) suggests the presence of the single type of PDGF or IFN- γ binding sites on DS-SILY₂₀ with dissociation constants on the same order as those found for DS and decorin. Consistent with the hypothesis that DS-SILY₂₀ is sequestering PDGF and IFN- γ , and thus, attenuating its impact on SMCs, the relative ratios of phosphorylated PDGF or IFN- γ receptors are decreased when PDGF- or IFN- γ -stimulated SMCs are also treated with 10 μ M DS-SILY₂₀, as compared to cultures stimulated with PDGF or IFN- γ alone

(Figure 2). While this is in contrast with work by Nili et al. showing that PDGF is able to bind both decorin and its receptor, the Nili et al. studies were performed using cell lysates rather than in a format where decorin could bind to a collagen matrix.¹⁹ In the present study, the DS-SILY₂₀ is able to bind to collagen surrounding the SMCs (Figure S4, Supporting Information), supporting the idea that collagen-bound DS-SILY₂₀ sequesters the PDGF making it unavailable to bind to its receptor.

SMC migration from the medial layer to the intimal layer, accompanied by increase protein synthesis within the intimal layer, is critical to intimal hyperplasia.⁵⁰ Previously, we demonstrated that proliferation, migration, and protein synthesis were significantly increased in proliferative SMC cultures.³⁶ We further demonstrated that DS-SILY₂₀ showed no negative impact on quiescent cells, as evidenced by little to no effect on protein synthesis, cell proliferation, or cell migration. However, DS-SILY₂₀ suppressed protein secretion, cell migration, and cell proliferation in proliferative cultures. Combined with the lack of effects on cell metabolism, this data supports the notion that DS-SILY₂₀ does not have deleterious effects on normal cell behavior, but suppresses behavior that leads to intimal thickening in proliferative SMCs.

In order to further evaluate the mechanism through which DS-SILY₂₀ suppressed intimal hyperplasia, we assessed the effects of DS-SILY₂₀ in PDGF stimulated morphological changes, proliferation, and migration in SMCs exhibiting either a proliferative or quiescent phenotype (Table 1; Figure 3).^{8,51} DS-SILY₂₀ was able to overcome morphological changes induced by PDGF in both proliferative and quiescent cultures (Figure S3, Supporting Information). Consistent with other studies, PDGF induced greater proliferation in quiescent cells than in proliferative cells, perhaps because the proliferative cells were already stimulated by factors present in the culture medium.⁵² Similarly, PDGF demonstrated an increased potency toward quiescent SMC migration. SMC migration has been correlated with pERK-1/2 levels. Consistent with the increased migration observed with PDGF stimulation in these studies, the relative levels of pERK-1/2 in quiescent cultures exhibited a larger fold increase compared to proliferative cultures (Figure 8).

Contrasting results were seen when stimulating with IFN- γ . Similar to results observed with PDGF, IFN- γ stimulated proliferation and migration in quiescent SMCs; however, it did stimulate changes in cell morphology, which was negated by treatment with DS-SILY₂₀ (Figure S3, Supporting Information). These confounding results between the two SMC phenotypes demonstrate the complex nature of IFN- γ signaling in tissue remodeling, adding to the conflicting reports depicting IFN- γ as both pro- and antirestenotic.^{16,17,53} Interestingly, the differential effects of IFN- γ have also been demonstrated elsewhere, where IFN- γ addition to quiescent SMCs resulted in increased proliferation and migration, while the growth factor had either no effect or reduced proliferation and protein synthesis in proliferative SMCs.^{8,12,53–56}

The addition of DS-SILY₂₀ to PDGF- or IFN- γ -stimulated SMCs correlated to a dose-dependent inhibition of SMC proliferation and migration in both SMC phenotypes, demonstrating that DS-SILY₂₀ retains bioactivity amidst the presence of growth factors. It is likely that DS-SILY₂₀ is able to block SMC stimulation by sequestering PDGF or IFN- γ , thus, limiting the stimuli's ability to activate or further promote restenotic SMC behavior in either injured and healthy SMC

phenotypes. Interestingly, higher concentrations of DS-SILY₂₀ were required to significantly reduce growth factor induced migration in quiescent SMCs compared to proliferative cultures. Increased concentrations of DS-SILY₂₀ were also required to mitigate increased relative levels of pERK-1/2 in growth factor-stimulated quiescent cultures; however, further investigation is needed to fully understand these findings.

Consistent with previous work and with the increased cell proliferation and migration observed here, PDGF stimulated protein synthesis in SMCs exhibiting either a proliferative or quiescent phenotype (Table 1). Again demonstrating that context is important in dictating whether IFN- γ is pro- or antiproliferative, IFN- γ stimulated protein synthesis in quiescent SMCs, the growth factor reduced protein synthesis in proliferative cultures. We speculate that the inconsistent results, demonstrated previously in literature, associating IFN- γ as both pro- and antiproliferative could be attributed to differences in cell physiology, as determined by the SMC phenotype utilized. The addition of DS-SILY₂₀ to PDGF- or IFN- γ -stimulated SMCs correlated to a dose-dependent inhibition of SMC protein synthesis in both SMC phenotypes. As we observed overall changes in protein synthesis, we hypothesized that we would observe changes in JNK phosphorylation, which has been correlated with collagen and fibronectin protein production.⁵⁷ Surprisingly, phosphorylation of JNK did not change when observed at 10 or 60 min post-treatment (data not shown). However, it is possible that the static phosphorylation studies did not capture the dynamic changes in JNK phosphorylation.

Since overall protein synthesis was increased in the proliferative phenotype and via stimulation with PDGF, we investigated whether ECM genes implicated in intimal hyperplasia were also upregulated. Both collagen I and fibronectin are upregulated in intimal hyperplasia, while collagen III is often down-regulated.^{58,59} While PDGF has been shown to stimulate collagen I, collagen III, and fibronectin production in SMCs, the growth factor did not induce collagen I, collagen III, or fibronectin gene expression in quiescent cultures in this investigation (Figure 4).^{51,60,61} In this study, PDGF stimulated quiescent SMC proliferation, which may shift expression toward essential cellular proteins and away from extracellular proteins. In fact, it has been demonstrated that the vast majority of cells exhibiting proliferative activity are not collagen-producing.⁶² This is in stark contrast with our results demonstrating that in proliferative SMCs stimulated with PDGF both an increase in proliferation and in collagen I and fibronectin gene expression were observed; however, this too is consistent with other studies.^{8,60} Furthermore, in the latter case, increased type I collagen gene expression may also be attributed to increased cytokine expression found in PDGF-stimulated proliferative SMC cultures.^{63,64} These results clearly show that environment and phenotypic state are critical factors in the complex responses to cell stimulation.

Following vessel injury, active SMCs participate in the inflammatory cycle by producing and secreting a range of pro-inflammatory factors, in response to mechanical and chemical stimuli.⁶⁵ It has previously been established that SMCs dosed with PDGF or IFN- γ exhibit an enhanced inflammatory response, a phenomenon we further demonstrate in this work.^{16,51} Consistent with studies demonstrating that DS-SILY₂₀ attenuates cytokine production in proliferative and quiescent SMC cultures, we reveal here that DS-SILY₂₀ reduces the production of pro-inflammatory cytokines secreted from PDGF- or IFN- γ -stimulated SMCs.³⁶ As expected, the addition

of 10 μ M DS-SILY₂₀ to PDGF- or IFN- γ -stimulated cultures decreased the production of all three inflammatory cytokines investigated (Figures 5 and 6). Interestingly, the treatment of cultures with PDGF or IFN- γ and low concentrations of DS-SILY₂₀ caused an increase of IL-1 β and TNF- α . Consistent with the increased IL-1 β and TNF- α production observed, the relative levels of pp38 also increased when stimulated with PDGF or IFN- γ coupled with low DS-SILY₂₀ concentrations (Figure 9). This observed increase in IL-1 β and TNF- α also corresponds with sustained migration and pERK-1/2 levels observed in quiescent SMCs under similar treatment conditions, indicating that low concentrations of the compound in the presence of chemical stimuli stimulates a small level of smooth muscle cell repair and remodeling.⁶⁶

In addition to the effect of DS-SILY₂₀ on growth factor-stimulated SMC cytokine production, the ability of this antithrombotic therapeutic to influence cellular expression of thrombomodulin is maintained in the presence of PDGF and IFN- γ . Thrombomodulin, a transmembrane glycoprotein, plays an important role in maintaining vascular thromboresistance as it forms a complex with thrombin, allowing for the activation of protein C and, thus, indirectly increasing fibrinolysis and inhibiting blood coagulation.⁶⁷ It has previously been determined that the overexpression of thrombomodulin, or similarly, the systemic administration of thrombomodulin, reduces inflammatory cell infiltration and neointimal formation in several animal models;^{68,69} thus, the ability to upregulate thrombomodulin in proliferative, unhealthy SMCs may serve as another important mechanism in the prevention of restenosis.

Thrombomodulin levels were significantly enhanced with the introduction of PDGF or IFN- γ to proliferative SMC cultures, attaining similar production levels to that of cultures treated with 10 μ M DS-SILY₂₀ alone (Figure 7). However, the lack of synergistic activity observed when proliferative cultures received cotreatments of PDGF or IFN- γ and high concentrations of DS-SILY₂₀ may be attributed to binding of PDGF and IFN- γ to the mimic, limiting the influence of the growth factors on cell behavior and as such that only the effects associated with DS-SILY₂₀ is observed. This claim is further strengthened by the fact that treatment with low concentrations of DS-SILY₂₀ and PDGF or IFN- γ resulted in decreased thrombomodulin production in proliferative cultures, similar to previous results observed with DS-SILY₂₀ alone.¹⁹ However, unlike in cultures treated with DS-SILY₂₀ alone, thrombomodulin production did not decrease below values observed in controls, indicating that the combination of certain growth factors with low concentrations of DS-SILY₂₀ may be useful for vessel remodeling and functional healing. Furthermore, while the upregulation of thrombomodulin may prove important in the treatment of proliferative, unhealthy SMCs, the ability to maintain quiescent, healthy SMC behavior is also important. Here, we demonstrate that the addition of PDGF or IFN- γ and DS-SILY₂₀ does not alter thrombomodulin production in quiescent SMCs, demonstrating that the therapeutic administration maintains quiescent SMC health.

Decorin has been shown to affect pathways in addition to PDGF and IFN- γ , perhaps most notably the TGF β -1 pathway.⁷⁰ With respect to TGF β -1, binding to decorin has been shown to be with the core protein rather than with the DS chain. Thus, it is unlikely that the activities seen here are due to altered TGF β -1 signaling. While we have demonstrated attenuation of PDGF and IFN- γ , it remains possible that DS-

SILY₂₀ binds to additional signaling molecules that also contribute to the observed activity.

CONCLUSION

We previously demonstrated that the decorin mimic, DS-SILY₂₀ suppressed intimal hyperplasia following balloon angioplasty at least in part through inhibition of platelet binding to the lumen of the denuded vessel. To further characterize the activity of DS-SILY₂₀ proliferative and quiescent cultures of SMCs were established, and the binding affinities of DS-SILY₂₀ with PDGF (32.2 ± 5.7 nM) and IFN- γ (55.1 ± 6.9 nM) were established. The nanomolar dissociation constants observed between DS-SILY₂₀ and both PDGF and IFN- γ , coupled with the ~ 24 nM dissociation constant between DS-SILY₂₀ and collagen, suggest that DS-SILY₂₀ is able to attenuate the effects of these factors, released from activated platelets, simply through sequestration. Consistent with this hypothesis, DS-SILY₂₀ attenuates the phosphorylation of the PDGF and IFN- γ receptors in the presence of PDGF or IFN- γ , respectively. In the case of PDGF, the growth factor significantly increased migration, proliferation, and protein and cytokine expression, as well as increased ERK-1/2 and p38 MAPK phosphorylation in both quiescent and proliferative cultures. In all cases, DS-SILY₂₀ inhibited these increases. Consistent with the complex responses seen with IFN- γ in SMC physiology in the literature, the response of SMC cultures to IFN- γ was variable and complex. However, where increased activity was seen with IFN- γ , DS-SILY₂₀ attenuated this activity. In no case did DS-SILY₂₀ abolish cell function, suggesting that while it is able to suppress intimal hyperplasia, it does not interfere with normal cell behavior and, hence, will not suppress healing associated with vessel injury. Furthermore, DS-SILY₂₀ had a positive influence on thrombomodulin expression, thereby making activated SMCs less thrombogenic. Overall, the results suggest that DS-SILY₂₀ would be an ideal alternative to traditional therapeutics used following PCI. The results warrant further characterization of DS-SILY₂₀ with endothelial cells to evaluate the ability of endothelial cell regrowth. This regrowth is inhibited by sirolimus and paclitaxel, which are commonly used to inhibit intimal hyperplasia following PCI; the lack of regrowth can lead to long-term issues including the need to systemically anticoagulate patients and the inability of the body to reestablish critical cell signaling between endothelial cells and smooth muscle cells.

ASSOCIATED CONTENT

Supporting Information

Metabolic activity of SMCs stimulated with PDGF, IFN- γ , and DS-SILY₂₀, viability of SMCs following treatment with PDGF, IFN- γ , and DS-SILY₂₀, representative images of SMC morphology poststimulation with PDGF, IFN- γ , and DS-SILY₂₀, representative images of DS-SILY₂₀ bound to ECM surrounding SMCs. This material is available free of charge via the Internet at <http://pubs.acs.org>.

AUTHOR INFORMATION

Corresponding Author

*Tel.: (765) 496-1313. Fax: (765) 496-1459. E-mail: apanitch@purdue.edu.

Notes

The authors declare the following competing financial interest(s): Alyssa Panitch owns greater than 5% of Symic

Biomedical, a company planning to enter into an agreement to license this technology from Purdue Research Foundation. This does not alter the authors' adherence to all the *Biomacromolecules* policies on sharing data and materials.

ACKNOWLEDGMENTS

Funding for this research was through NIH R01HL106792. R.A.S. is supported by a NSF Graduate Research Fellowship (DGE-1333468).

REFERENCES

- (1) Buie, V. C.; Owings, M. F.; DeFrances, C. J.; Golosinskiy, A. *National Hospital Discharge Survey: 2006 Summary*; National Center For Health Statistics: Hyattsville, MD, 2010; Vol. 13.
- (2) Lloyd-Jones, D.; Adams, R.; Carnethon, M.; De Simone, G.; Ferguson, T. B.; Flegal, K.; Ford, E.; Furie, K.; Go, A.; Greenlund, K.; Haase, N.; Hailpern, S.; Ho, M.; Howard, V.; Kissela, B.; Kittner, S.; Lackland, D.; Lisabeth, L.; Marelli, A.; McDermott, M.; Meigs, J.; Mozaffarian, D.; Nichol, G.; O'Donnell, C.; Roger, V.; Rosamond, W.; Sacco, R.; Sorlie, P.; Stafford, R.; Steinberger, J.; Thom, T.; Wasserthiel-Smoller, S.; Wong, N.; Wylie-Rosett, J.; Hong, Y. American Heart Association Statistics Committee and Stroke Statistics. *Circulation* **2008**, *119*, 1–161.
- (3) American Heart Association *Heart Disease and Stroke Statistics - 2010 Update*; American Heart Association: Dallas, TX, 2010.
- (4) Karas, S. P.; Gravanis, M. B.; Santoian, E. C.; Robinson, K. A.; Anderberg, K. A.; King Iii, S. B. *J. Am. Coll. Cardiol.* **1992**, *20* (2), 467–474.
- (5) MacLeod, D. C.; Strauss, B. H.; de Jong, M.; Escaned, J.; Umans, V. A.; van Suylen, R. J.; Verkerk, A.; de Feyter, P. J.; Serruys, P. W. *J. Am. Coll. Cardiol.* **1994**, *23* (1), 59–65.
- (6) Hanke, H.; Strohschneider, T.; Oberhoff, M.; Betz, E.; Karsch, K. *Circ. Res.* **1990**, *67* (3), 651–659.
- (7) Loppnow, H.; Bil, R.; Hirt, S.; Schonbeck, U.; Herzberg, M.; Werdan, K.; Theodor Rietschel, E.; Brandt, E.; Flad, H. D. *Blood* **1998**, *91* (1), 134–141.
- (8) Amento, E. P.; Ehsani, N.; Palmer, H.; Libby, P. *Arterioscler. Thromb. Vasc. Biol.* **1991**, *11* (5), 1223–30.
- (9) Jackson, C. L.; Raines, E. W.; Ross, R.; Reidy, M. A. *Arterioscler. Thromb. Vasc. Biol.* **1993**, *13* (8), 1218–26.
- (10) Jovinge, S.; Hultgårdh-Nilsson, A.; Regnström, J.; Nilsson, J. *Arterioscler. Thromb. Vasc. Biol.* **1997**, *17* (3), 490–497.
- (11) Jiang, B.; Yamamura, S.; Nelson, P. R.; Mureebe, L.; Kent, K. C. *Surgery* **1996**, *120* (2), 427–432.
- (12) Amrani, Y.; Tliba, O.; Choubey, D.; Huang, C.-D.; Krymskaya, V. P.; Eszterhas, A.; Lazaar, A. L.; Panettieri, R. A. *Am. J. Physiol.: Lung Cell. Mol. Physiol.* **2003**, *284* (6), L1063–L1071.
- (13) Smith, M. A.; Moylan, J. S.; Smith, J. D.; Li, W.; Reid, M. B. *Am. J. Physiol.: Cell Physiol.* **2007**, *293* (6), C1947–C1952.
- (14) Jawien, A.; Bowen-Pope, D. F.; Lindner, V.; Schwartz, S. M.; Clowes, A. W. *J. Clin. Invest.* **1992**, *89* (2), 507–11.
- (15) Miyauchi, K.; Aikawa, M.; Tani, T.; Nakahara, K.; Kawai, S.; Nagai, R.; Okada, R.; Yamaguchi, H. *Cardiovasc. Drugs Ther.* **1998**, *12* (3), 251–60.
- (16) Harvey, E. J.; Ramji, D. P. *Cardiovasc. Res.* **2005**, *67* (1), 11–20.
- (17) Wang, Y.; Bai, Y.; Qin, L.; Zhang, P.; Yi, T.; Teesdale, S. A.; Zhao, L.; Pober, J. S.; Tellides, G. *Circ. Res.* **2007**, *101* (6), 560–569.
- (18) Camejo, E. H.; Rosengren, B.; Camejo, G.; Sartipy, P.; Fager, G.; Bondjers, G. *Arterioscler. Thromb. Vasc. Biol.* **1995**, *15* (9), 1456–1465.
- (19) Nili, N.; Cheema, A. N.; Giordano, F. J.; Barolet, A. W.; Babaei, S.; Hickey, R.; Eskandarian, M. R.; Smeets, M.; Butany, J.; Pasterkamp, G.; Strauss, B. H. *Am. J. Pathol.* **2003**, *163* (3), 869–878.
- (20) Riessen, R.; Isner, J.; Blessing, E.; Loushin, C.; Nikol, S.; Wight, T. *Am. J. Pathol.* **1994**, *144*, 962–974.
- (21) Salisbury, B. G.; Wagner, W. D. *J. Biol. Chem.* **1981**, *256* (15), 8050–7.

- (22) Fiedler, L. R.; Schonherr, E.; Waddington, R.; Niland, S.; Seidler, D. G.; Aeschlimann, D.; Eble, J. A. *J. Biol. Chem.* **2008**, *283*, 17406–17415.
- (23) Hildebrand, A.; Romaris, M.; Rasmussen, M.; Heinegard, D.; Twardzik, D. R.; Border, W. A.; Ruoslahti, E. *Biochem. J.* **1994**, *302* (2), 527–534.
- (24) De Luca, A.; Santra, M.; Baldi, A.; Giordano, A.; Iozzo, R. V. *J. Biol. Chem.* **1996**, *271* (31), 18961–18965.
- (25) Fischer, J. W.; Kinsella, M. G.; Levkau, B.; Clowes, A. W.; Wight, T. N. *Arterioscler. Thromb. Vasc. Biol.* **2001**, *21* (5), 777–784.
- (26) Winnemöller, M.; Schön, P.; Vischer, P.; Kresse, H. *Eur. J. Cell Biol.* **1992**, *59* (1), 47–55.
- (27) Seidler, D. G.; Goldoni, S.; Agnew, C.; Cardì, C.; Thakur, M. L.; Owens, R. T.; McQuillan, D. J.; Iozzo, R. V. *J. Biol. Chem.* **2006**, *281* (36), 26408–26418.
- (28) Hikino, M.; Mikami, T.; Faissner, A.; Vilela-Silva, A.-C. E. S.; Pavão, M. S. G.; Sugahara, K. *J. Biol. Chem.* **2003**, *278* (44), 43744–43754.
- (29) Penc, S. F.; Pomahac, B.; Winkler, T.; Dorschner, R. A.; Eriksson, E.; Herndon, M.; Gallo, R. L. *J. Biol. Chem.* **1998**, *273* (43), 28116–28121.
- (30) Kozma, E. M.; Wisowski, G.; Olczyk, K. *Biochimie* **2009**, *91* (11,12), 1394–1404.
- (31) Brooks, B.; Briggs, D. M.; Eastmond, N. C.; Fernig, D. G.; Coleman, J. W. *J. Immunol.* **2000**, *164* (2), 573–579.
- (32) Cella, G.; Boeri, G.; Saggiorato, G.; Paolini, R.; Luzzatto, G.; Terribile, V. I. *Angiology* **1992**, *43* (1), 59–62.
- (33) Trowbridge, J. M.; Gallo, R. L. *Glycobiology* **2002**, *12* (9), 117R–125R.
- (34) Paderi, J. E.; Panitch, A. *Biomacromolecules* **2008**, *9* (9), 2562–2566.
- (35) Paderi, J. E.; Stuart, K.; Sturek, M.; Park, K.; Panitch, A. *Biomaterials* **2011**, *32* (10), 2516–2523.
- (36) Scott, R. A.; Paderi, J. E.; Sturek, M.; Panitch, A. *PLoS One* **2013**, *8* (11), e82456.
- (37) Chaterji, S.; Park, K.; Panitch, A. *Tissue Eng., Part A* **2010**, *16* (6), 1901–1912.
- (38) Beatty, K. E.; Liu, J. C.; Xie, F.; Dieterich, D. C.; Schuman, E. M.; Wang, Q.; Tirrell, D. A. *Angew. Chem., Int. Ed.* **2006**, *45* (44), 7364–7367.
- (39) Hedbom, E.; Heinegard, D. *J. Biol. Chem.* **1989**, *264* (12), 6898–6905.
- (40) Boyden, S. J. *Exp. Med.* **1962**, *115* (3), 453–466.
- (41) Izumi, Y.; Kim, S.; Namba, M.; Yasumoto, H.; Miyazaki, H.; Hoshiga, M.; Kaneda, Y.; Morishita, R.; Zhan, Y.; Iwao, H. *Circ. Res.* **2001**, *88* (11), 1120–1126.
- (42) Xu, Q.; Liu, Y.; Gorospe, M.; Udelsman, R.; Holbrook, N. J. *J. Clin. Invest.* **1996**, *97* (2), 508–514.
- (43) Force, T.; Pombo, C. M.; Avruch, J. A.; Bonventre, J. V.; Kyriakis, J. M. *Circ. Res.* **1996**, *78* (6), 947–953.
- (44) Zhan, Y.; Kim, S.; Izumi, Y.; Izumiya, Y.; Nakao, T.; Miyazaki, H.; Iwao, H. *Arterioscler. Thromb. Vasc. Biol.* **2003**, *23* (5), 795–801.
- (45) Liu, N.; Liu, J.; Ji, Y.; Lu, P.; Wang, C.; Guo, F. *Inflammation* **2011**, *34* (4), 283–290.
- (46) Carter, A. B.; Monick, M. M.; Hunninghake, G. W. *Am. J. Respir. Cell Mol. Biol.* **1999**, *20* (4), 751–758.
- (47) van den Blink, B.; Juffermans, N. P.; ten Hove, T.; Schultz, M. J.; van Deventer, S. J. H.; van der Poll, T.; Peppelenbosch, M. P. *J. Immunol.* **2001**, *166* (1), 582–587.
- (48) Nobuyoshi, M.; Kimura, T.; Nosaka, H.; Mioka, S.; Ueno, K.; Yokoi, H.; Hamasaki, N.; Horiuchi, H.; Ohishi, H. *J. Am. Coll. Cardiol.* **1988**, *12* (3), 616–623.
- (49) Hedbom, E.; Heinegård, D. *J. Biol. Chem.* **1989**, *264* (12), 6898–6905.
- (50) Nobuyoshi, M.; Kimura, T.; Ohishi, H.; Horiuchi, H.; Nosaka, H.; Hamasaki, N.; Yokoi, H.; Kim, K. *J. Am. Coll. Cardiol.* **1991**, *17* (2), 433–439.
- (51) Deng, D. X.-F.; Spin, J. M.; Tsalenko, A.; Vailaya, A.; Ben-Dor, A.; Yakhini, Z.; Tsao, P.; Bruhn, L.; Quatermous, T. *Arterioscler. Thromb. Vasc. Biol.* **2006**, *26* (5), 1058–1065.
- (52) Wang, W.; Chen, H. J.; Giedd, K. N.; Schwartz, A.; Cannon, P. J.; Rabbani, L. E. *Circ. Res.* **1995**, *77* (6), 1095–1106.
- (53) Yokota, T.; Shimokado, K.; Kosaka, C.; Sasaguri, T.; Masuda, J.; Ogata, J. *Arterioscler. Thromb. Vasc. Biol.* **1992**, *12* (12), 1393–401.
- (54) Hansson, G. K.; Jonasson, L.; Holm, J.; Clowes, M. M.; Clowes, A. W. *Circ. Res.* **1988**, *63* (4), 712–9.
- (55) Song, Y. L.; Ford, J. W.; Gordon, D.; Shanley, C. J. *Arterioscler. Thromb. Vasc. Biol.* **2000**, *20* (4), 982–988.
- (56) Yu, L.; Qin, L.; Zhang, H.; He, Y.; Chen, H.; Pober, J. S.; Tellides, G.; Min, W. *Circ. Res.* **2011**, *109* (4), 418–427.
- (57) González-Ramos, M.; Calleros, L.; López-Ongil, S.; Raoch, V.; Griera, M.; Rodríguez-Puyol, M.; de Frutos, S.; Rodríguez-Puyol, D. *Int. J. Biochem. Cell Biol.* **2013**, *45* (2), 232–242.
- (58) Coats, W. D.; Cheung, D. T.; Han, B.; Currier, J. W.; Faxon, D. P. *J. Mol. Cell. Cardiol.* **1996**, *28* (2), 441–446.
- (59) Clausell, N.; de Lima, V. C.; Molossi, S.; Liu, P.; Turley, E.; Gottlieb, A. I.; Adelman, A. G.; Rabinovitch, M. *Br. Heart J.* **1995**, *73* (6), 534–539.
- (60) Yang, F.; Zhao, P.; She, M.; Ye, G.; Han, X. *Zhongguo Yi Xue Ke Xue Yuan Xue Bao* **1999**, *21* (1), 13–8.
- (61) Lo, C.-S.; Tamaroglio, T.; Zhang, J. *J. Biomed. Sci.* **1995**, *2* (1), 63–69.
- (62) Reikter, M. D. *Cardiovasc. Res.* **1999**, *41* (2), 376–384.
- (63) Asselot-Chapel, C.; Combacau, L.; Labat-Robert, J.; Kern, P. *Biochem. Pharmacol.* **1995**, *49* (5), 653–659.
- (64) Hsu, J.-Y.; Hsu, M.-Y.; Sorger, T.; Herlyn, M.; Levine, E. M. *In Vitro Cell. Dev. Biol.: Anim.* **1999**, *35* (10), 647–654.
- (65) Sukkar, M. B.; Stanley, A. J.; Blake, A. E.; Hodgkin, P. D.; Johnson, P. R. A.; Armour, C. L.; Hughes, J. M. *Immunol. Cell Biol.* **2004**, *82* (5), 471–478.
- (66) Sanchez-Guerrero, E.; Chen, E.; Kockx, M.; An, S.-W.; Chong, B. H.; Khachigian, L. M. *PLoS One* **2012**, *7* (7), e39811.
- (67) Wen, D.; Dittman, W. A.; Ye, R. D.; Deaven, L. L.; Majerus, P. W.; Sadler, J. E. *Biochemistry* **1987**, *26* (14), 4350–4357.
- (68) Waugh, J. M.; Li-Hawkins, J.; Yuksel, E.; Kuo, M. D.; Cifra, P. N.; Hilfiker, P. R.; Geske, R.; Chawla, M.; Thomas, J.; Shenaq, S. M.; Dake, M. D.; Woo, S. L. C. *Circulation* **2000**, *102* (3), 332–337.
- (69) Li, J. M.; Singh, M. J.; Itani, M.; Vasiliu, C.; Hendricks, G.; Baker, S. P.; Hale, J. E.; Rohrer, M. J.; Cutler, B. S.; Nelson, P. R. *J. Vasc. Surg.* **2004**, *39* (5), 1074–1083.
- (70) Schönherr, E.; Broszat, M.; Brandan, E.; Bruckner, P.; Kresse, H. *Arch. Biochem. Biophys.* **1998**, *355* (2), 241–248.